Pure-Cubic Optical Solitons With Kerr Law By Laplace-Adomian Decomposition

O. Gonzalez-Gaxiola[1], Anjan Biswas[2,3,4,5], Yakup Yıldırım[6,7], and Asim Asiri[3]

[1] *Applied Mathematics and Systems Department, Universidad Autonoma Metropolitana–Cuajimalpa, Vasco de Quiroga 4871, 05348 Mexico City, Mexico*
[2] *Department of Mathematics and Physics, Grambling State University, Grambling, LA 71245–2715, USA*
[3] *Mathematical Modeling and Applied Computation (MMAC) Research Group, Center of Modern Mathematical Sciences and their Applications (CMMSA), Department of Mathematics, King Abdulaziz University, Jeddah—21589, Saudi Arabia*
[4] *Department of Applied Sciences, Cross—Border Faculty of Humanities, Economics and Engineering, Dunarea de Jos University of Galati, 111 Domneasca Street, Galati—800201, Romania*
[5] *Department of Mathematics and Applied Mathematics, Sefako Makgatho Health Sciences University, Medunsa—0204, Pretoria, South Africa*
[6] *Department of Computer Engineering, Biruni University, Istanbul 34010, Turkey*
[7] *Department of Mathematics, Near East University, 99138 Nicosia, Cyprus*
[*] *Corresponding author. E-mail: biswas.anjan@gmail.com*

Received: Jul.05, 2023; Accepted: Oct.26, 2023

This paper retrieves pure-cubic optical solitons for the nonlinear Schrödinger's equation when chromatic dispersion term is dropped due to its low count. This model with the inclusion of third-order dispersion after dropping chromatic dispersion maintains the necessary balance between dispersion and self-phase modulation for the solitons to sustain. The Laplace-Adomian decomposition scheme is applied to recover such pure-cubic soliton solutions. The surface plots as well as the contour plots for bright and dark soliton solutions are displayed. The results are profoundly significant and novel. The numerical simulation for pure-cubic solitons is being reported for the very first time in this paper. While in the past, solitons were studied with chromatic dispersion, this is the first-time solitons are being addressed, and that too numerically, with pure-cubic dispersion format. The radiation effects are ignored to focus on the core soliton regime. The results are impressive and promising. The two-dimensional numerical simulation and the exact solutions to the model are almost a perfect match. The error table displays a measure of the order of 10^{-7}.

Keywords: Pure-cubic optical solitons; Generalized third order NLSE; Cubic nonlinearity; Laplace-Adomian decomposition method

http://dx.doi.org/10.6180/jase.202410_27(10).0003

1. Introduction

The nonlinear Schrodinger's equation is the standard model for studying the propagation of solitons through optical fibers, metamaterials, and other forms of optical waveguide. This equation comprises of three important terms. They are the linear temporal evolution, chromatic dispersion (CD) and the nonlinear term that is from Kerr law which accounts for self-phase modulation (SPM). The solitons result from a delicate equilibrium between CD and SPM.

Occasionally, it can so happen that the CD runs low. In that case, the equilibrium between CD and SPM has been compromised. The consequential pulse collapse is inevitable. In order to avoid such an impending catastro-

phe, the low count CD is replaced with the third-order dispersion (3OD). The solitons that are thus produced are referred to as pure-cubic solitons. The current paper retrieves the pure-cubic bright and dark soliton solutions to the model with a couple of perturbation terms taken into consideration. The inclusion of the two Hamiltonian type perturbation terms is justified for integrability purposes. The unperturbed version of NLSE with CD replaced by 3OD is not rendered to be integrable, since it will not pass the Painlevé test. Therefore, to salvage the integrability of the NLSE, the Hamiltonian perturbation terms are included. These two perturbative effects are from self-frequency shift. The main reason for this study stems from the extensive theoretical and experimental investigations conducted over a duration of more than 50 years, which have shown the significant role of solitons in the realm of nonlinear wave mechanics. The nonlinear Schrödinger equation is of significant practical importance due to its involvement in the self-focusing phenomenon observed in non-linear media [1]. This phenomenon occurs during the continuous propagation of non-propagating electromagnetic pulses.

Laplace-Adomian decomposition technique is the integration scheme. Both bright and dark soliton solutions are recovered using the scheme. The recovered numerical results are compared with the recovered analytical approaches [2]. The match is almost exact. The surface plots of bright and dark solitons are displayed along with their respective contour plots. The error measure is presented is a range of tables where it shows that this impressive count is of the order of 10^{-7}. After a succinct introduction to the model and a review of the model's reported results, the remainder of the paper presents the specific details.

2. Mathematical expression of the model

We analyze the movement of a very bright light pulse through an optical waveguide, where the evolution of the pulse is controlled by the generalized third-order nonlinear Schrödinger equation [3–6]:

$$\begin{aligned} &iq_t + iaq_{xxx} + b|q|^2 q = \\ &i\left[\sigma_1|q|^2 q_x + \sigma_2\left(|q|^2\right)_x q\right], \end{aligned} \tag{1}$$

where q represents a complex function that is dependent on the temporal variable t and the spatial variable x; a represents a coefficient of 3OD, the cubic nonlinearity is governed by b, meanwhile the dispersive terms are controlled by σ_1 and σ_2. By assuming $\sigma_1 = \sigma_2 = 0$, Eq. (1) is transformed into the modified KdV equation, the integrability of which may be determined by the inverse scattering transform.

The nonlinear Schrodinger Eq. (1) hold considerable importance within the context of nonlinear evolution equations, as they appear in various scientific fields including optical fibers, hydrodynamics, biology, elastic media, quantum mechanics, magneto-static rotating waves, and optics, among others. This field of study is now experiencing significant research activity, with many researchers being actively involved in investigating this specific direction [7–11].

The preceding model has been explored by a variety of authors using different methodologies. For instance, in [3], the authors obtain several families of solitons using the exp-expansion and extended simple equation techniques, in [4], the authors report multiple families of solitons using the modified Riccati approach, the authors of [5] have been able to obtain many families of solutions by using a variety of analytical techniques, auxiliary equation type strategies were used to analyze in [6], and in [12], elliptic solutions for the same model are obtained. In [13], the model was also researched using fractional derivatives.

3. Bright and dark solitons of Eq. (1) obtained using LADM

3.1. Overview of the Method

The proposed technique, known as the Laplace-Adomian decomposition method (LADM), was originally implemented in 1986 by G. Adomian and R. Rach [14]. LADM is based on the Adomian decomposition method and the Laplace transform. This method allows numerical solutions to be described as a quickly convergent series [15].

Consider a general nonlinear partial differential equation, given in symbolic form as:

$$Fq(x,t) = 0, \tag{2}$$

subject to initial condition

$$q(x,0) = f(x). \tag{3}$$

The differential operator F in Eq. (2) may be written as $F = L_t - R - N$, where $L_t q = q_t$. The nonlinear component and the linear operator are denoted by N and R, respectively. In general, Eq. (2) may be represented as

$$L_t q(x,t) = Rq(x,t) + Nq(x,t). \tag{4}$$

Through the application of the Laplace transform and its well-known transform over a time derivative property, $\mathcal{L}\{q_t(x,t)\} = s\mathcal{L}\{q(x,t)\} - q(x,0)$, the Eq. (4) might be rewritten as

$$sq(x,s) - q(x,0) = \mathcal{L}\{Rq(x,t) + Nq(x,t)\}. \tag{5}$$

Taking into account the initial condition in Eq. (3), we have

$$q(x,s) = \frac{f(x)}{s} + \frac{1}{s}\mathcal{L}\{Rq(x,t) + Nq(x,t)\}. \tag{6}$$

Applying the inverse Laplace transform $\mathcal{L}^{-1}$ to both sides of the equation allows for the easy determination of the dependent variable $q(x,t)$:

$$q(x,t) = f(x) + \mathcal{L}^{-1}\left[\frac{1}{s}\mathcal{L}\{Rq(x,t) + Nq(x,t)\}\right]. \tag{7}$$

The approach assumes that the unknown function q may be decomposed into a series of functions, and the nonlinear component N can be decomposed into a series of Adomian polynomials. The respective decompositions are as follows:

$$q(x,t) = \sum_{n=0}^{\infty} q_n(x,t). \tag{8}$$

$$Nq(x,t) = \sum_{n=0}^{\infty} P_n\left(q_0, q_1, \ldots, q_n\right), \tag{9}$$

where $\{P_n\}_{n=0}^{\infty}$ is the series of so-called Adomian polynomials. The following formula will be used to get the Adomian polynomial P_n for any nonlinear function [16]:

$$P_n\left(q_0, \ldots, q_n\right) = \begin{cases} N\left(q_0\right) & \text{if } n = 0 \\ \frac{1}{n}\sum_{k=0}^{n-1}(k+1)q_{k+1}\frac{\partial}{\partial q_0}P_{n-1-k} & \text{if } n \geq 1. \end{cases} \tag{10}$$

Substituting Eqs. (8) and (9) into Eq. (7) gives rise to

$$\sum_{n=0}^{\infty} q_n(x,t) = f(x) + \mathcal{L}^{-1}\left[\frac{1}{s}\left(\mathcal{L}\left\{R\left(\sum_{n=0}^{\infty} q_n(x,t)\right)\right\} + \mathcal{L}\left\{\sum_{n=0}^{\infty} P_n\left(q_0, \ldots, q_n\right)\right\}\right)\right]. \tag{11}$$

The components of the series (8), derived from the Eq. (11), are computed using the following algorithm, for every $n = 0, 1, 2, \ldots$:

$$\begin{cases} q_0(x,t) = f(x), \\ q_{n+1}(x,t) = \mathcal{L}^{-1}\left[\frac{1}{s}\mathcal{L}\left\{Rq_n(x,t) + P_n\left(q_0, q_1, \ldots, q_n\right)\right\}\right]. \end{cases} \tag{12}$$

Hence, the explicit solution of Eq. (2) is written as follows:

$$q(x,t) = \sum_{n=0}^{\infty} q_n(x,t). \tag{13}$$

Finally, a numerical approximation to K-terms will be given by the partial sum

$$q_K(x,t) = \sum_{n=0}^{K-1} q_n(x,t), \quad K \geq 1. \tag{14}$$

Principal highlight of LADM is its immediate applicability to all differential equation types, whether linear or nonlinear, ordinary or partial, homogeneous or inhomogeneous, and with constant or variable coefficients. Importantly, the LADM can solve nonlinear problems without linearization, discretization, or perturbed parameters [17]. However, the LADM has limitations, as we know that this method provides an approximation of the solution to the problem through a series of functions. The difficulty may be the region and rate of convergence of the series solution. As the resulting series may be rapidly convergent in a very small region, but has a slow convergence rate in wider regions, the approximated series is an unacceptable solution in this region, thereby restricting the method's applicability [18].

Now we will implement the LADM-supplied technique to solve the generalized third-order nonlinear Schrodinger Eq. (1).

3.2. Application of the Method for Eq. (1)

The following notation is used to implement this approach for solving the generalized third-order nonlinear Schrodinger Eq. (1):

$$L_t q = Nq + Rq, \tag{15}$$

where, the differential operators N and R act on u as

$$\begin{aligned} Nq &= ib|q|^2 q + \sigma_1|q|^2 q_x + \sigma_2\left(|q|^2\right)_x q, \\ Rq &= -aq_{xxx}. \end{aligned} \tag{16}$$

The nonlinear differential operator N may be divided into the following parts:

$$Nu = \left(N_1 + N_2 + N_3\right) q, \tag{17}$$

considering:

$$\begin{aligned} N_1 u &= ib|u|^2 q, \\ N_2 q &= \sigma_1|q|^2 q_x, \\ N_3 q &= \sigma_2\left(|q|^2\right)_x u. \end{aligned} \tag{18}$$

According to the formula Eq. (9), the nonlinear parts are decomposed into Adomian polynomials as follows

$$\begin{aligned} N_1 q &= ib|q|^2 q \\ &= \sum_{n=0}^{\infty} A_n\left(q_0, q_1, \ldots, q_n\right) \end{aligned} \tag{19}$$

$$N_2 q = \sigma_1 |q|^2 q_x = \sum_{n=0}^{\infty} B_n (q_0, q_1, \ldots, q_n), \tag{20}$$

and

$$N_3 u = \sigma_2 \left(|q|^2\right)_x q = \sum_{n=0}^{\infty} C_n (q_0, q_1, \ldots, q_n). \tag{21}$$

In order to get the adomian polynomials A_n, B_n, and C_n, we may use the formula given by Eq. (10), that is,

$$A_0 = N_1 (q_0), \quad B_0 = N_2 (q_0), \quad C_0 = N_3 (q_0), \tag{22}$$

and

$$A_n = \frac{1}{n} \sum_{k=0}^{n-1} (k+1) q_{k+1} \frac{\partial}{\partial q_0} A_{n-1-k}, \quad n \geq 1, \tag{23}$$

$$B_n = \frac{1}{n} \sum_{k=0}^{n-1} (k+1) q_{k+1} \frac{\partial}{\partial q_0} B_{n-1-k}, \quad n \geq 1, \tag{24}$$

$$C_n = \frac{1}{n} \sum_{k=0}^{n-1} (k+1) q_{k+1} \frac{\partial}{\partial q_0} C_{n-1-k}, \quad n \geq 1. \tag{25}$$

A few of the first Adomian polynomials are given by

$$\begin{aligned}
A_0 &= ibq_0^2 \bar{q}_0, \\
A_1 &= ib \left(2q_0 q_1 \bar{q}_0 + q_0^2 \bar{q}_1\right), \\
A_2 &= ib \left(2q_0 q_2 \bar{q}_0 + q_1^2 \bar{q}_0 + 2q_0 q_1 \bar{q}_1 + q_0^2 \bar{q}_2\right), \\
A_3 &= ib \left(2q_0 q_3 \bar{q}_0 + 2q_1 q_2 \bar{q}_0 + 2q_0 q_2 \bar{q}_1 + q_1^2 \bar{q}_1 + 2q_0 q_1 \bar{q}_2 + q_0^2 \bar{q}_3\right), \\
A_4 &= ia_1 \left(\bar{q}_0 q_2^2 + 2q_0 \bar{q}_0 q_4 + 2\bar{q}_0 q_1 q_3 + 2q_0 \bar{q}_1 q_3 + 2q_1 \bar{q}_1 q_2 + 2q_0 \bar{q}_2 q_2 + q_1^2 \bar{q}_2 + 2q_0 \bar{q}_1 q_3 + q_0^2 \bar{q}_4\right), \\
&\vdots
\end{aligned}$$

$$\begin{aligned}
B_0 &= \sigma_1 q_0 \bar{q}_0 q_{0x}, \\
B_1 &= \sigma_1 \left(q_0 \bar{q}_0 q_{1x} + q_0 \bar{q}_1 q_{0x} + q_1 \bar{q}_0 q_{0x}\right), \\
B_2 &= \sigma_1 \left(q_0 \bar{q}_0 q_{2x} + q_0 \bar{q}_1 q_{1x} + q_0 \bar{q}_2 q_{0x} + q_1 \bar{q}_0 q_{1x} + q_1 \bar{q}_1 q_{0x} + q_2 \bar{q}_0 q_{0x}\right), \\
B_3 &= \sigma_1 \left(q_0 \bar{q}_0 q_{3x} + q_0 \bar{q}_1 q_{2x} + q_0 \bar{q}_2 q_{1x} + q_0 \bar{q}_3 q_{0x} + q_1 \bar{q}_0 q_{2x} + q_1 \bar{q}_1 q_{1x} + q_1 \bar{q}_2 q_{0x} + q_2 \bar{q}_0 q_{1x} + q_2 \bar{q}_1 q_{0x} + q_3 \bar{q}_0 q_{0x}\right), \\
B_4 &= \sigma_1 \left(q_0 \bar{q}_0 q_{4x} + q_0 \bar{q}_1 q_{3x} + q_0 \bar{q}_2 q_{2x} + q_0 \bar{q}_3 q_{1x} + q_0 \bar{q}_4 q_{0x} + q_1 \bar{q}_0 q_{3x} + q_1 \bar{q}_1 q_{2x} + q_1 \bar{q}_2 q_{1x} + q_1 \bar{q}_3 q_{0x} + q_2 \bar{q}_0 q_{2x} + q_2 \bar{q}_1 q_{1x} + q_2 \bar{q}_2 q_{0x} + q_3 \bar{q}_0 q_{1x} + q_3 \bar{q}_1 q_{0x} + q_4 \bar{q}_0 q_{0x}\right), \\
&\vdots
\end{aligned}$$

$$\begin{aligned}
C_0 &= \sigma_2 \left(q_0^2 \bar{q}_{0x} + q_0 \bar{q}_0 q_{0x}\right), \\
C_1 &= \sigma_2 \left(2q_0 q_1 \bar{q}_{0x} + q_0^2 \bar{q}_{1x} + q_0 \bar{q}_0 q_{1x} + q_0 \bar{q}_1 q_{0x} + q_1 \bar{q}_0 q_{0x}\right), \\
C_2 &= \sigma_2 \left(2q_0 q_2 \bar{q}_{0x} + q_1^2 \bar{q}_{0x} + 2q_0 q_1 \bar{q}_{1x} + q_0^2 \bar{q}_{2x} + q_0 \bar{q}_0 q_{2x} + q_0 \bar{q}_1 q_{1x} + q_0 \bar{q}_2 q_{0x} + q_1 \bar{q}_0 q_{1x} + q_1 \bar{q}_1 q_{0x} + q_2 \bar{q}_0 q_{0x}\right), \\
C_3 &= \sigma_2 \left(2q_0 q_3 \bar{q}_{0x} + 2q_1 q_2 \bar{q}_{0x} + 2q_0 q_2 \bar{q}_{1x} + q_1^2 \bar{q}_{1x} + 2q_0 q_1 \bar{q}_{2x} + q_0^2 \bar{q}_{3x} + q_0 \bar{q}_0 q_{3x} + q_0 \bar{q}_1 q_{2x} + q_0 \bar{q}_2 q_{1x} + q_0 \bar{q}_3 q_{0x} + q_1 \bar{q}_0 q_{2x} + q_1 \bar{q}_1 q_{1x} + q_1 \bar{q}_2 q_{0x} + q_2 \bar{q}_0 q_{1x} + q_2 \bar{q}_1 q_{0x} + q_3 \bar{q}_0 q_{0x}\right), \\
C_4 &= \sigma_2 \left(\bar{q}_{0x} q_2^2 + 2q_0 \bar{q}_{0x} q_4 + 2\bar{q}_{0x} q_1 q_3 + 2q_0 \bar{q}_{1x} q_3 + 2q_1 \bar{q}_{1x} q_2 + 2q_0 \bar{q}_{2x} q_2 + q_1^2 \bar{q}_{2x} + 2q_0 \bar{q}_{1x} q_3 + q_0^2 \bar{q}_{4x} + q_0 \bar{q}_0 q_{4x} + q_0 \bar{q}_1 q_{3x} + q_0 \bar{q}_2 q_{2x} + q_0 \bar{q}_3 q_{1x} + q_0 \bar{q}_4 q_{0x} + q_1 \bar{q}_0 q_{3x} + q_1 \bar{q}_1 q_{2x} + q_1 \bar{q}_2 q_{1x} + q_1 \bar{q}_3 q_{0x} + q_2 \bar{q}_0 q_{2x} + q_2 \bar{q}_1 q_{1x} + q_2 \bar{q}_2 q_{0x} + q_3 \bar{q}_0 q_{1x} + q_3 \bar{q}_1 q_{0x} + q_4 \bar{q}_0 q_{0x}\right), \\
&\vdots
\end{aligned}$$

Eq. (12) provides a recurrence relation, from which we can retrieve the following components:

$$
\begin{aligned}
&q_0(x,t) = f(x),\\
&q_1(x,t) = \\
&\quad \mathcal{L}^{-1}\left[\frac{1}{s}\mathcal{L}\left\{Rq_0(x,t) + (A_0 + B_0 + C_0)\,(q_0)\right\}\right],\\
&q_2(x,t) = \\
&\quad \mathcal{L}^{-1}\left[\frac{1}{s}\mathcal{L}\left\{Rq_1(x,t) + (A_1 + B_1 + C_1)\,(q_0,q_1)\right\}\right], \qquad (26)\\
&\vdots\\
&q_K(x,t) = \mathcal{L}^{-1}\left[\frac{1}{s}\mathcal{L}\left\{Rq_{K-1}(x,t) + (A_{K-1} + B_{N-1}\right.\right.\\
&\quad \left.\left.+C_{K-1})\,(q_0,q_1,\ldots,q_{K-1})\right\}\right].
\end{aligned}
$$

The above methodology will be shown with examples in the section that follows.

4. Graphical representations of the results of numerical simulations

4.1. Pure-Cubic Dark Solitons

Consider the following cases of Eq. (1) with the given set of parameters: Set $A : a = 1.0, b = 0.5, \sigma_1 = 4.3, \sigma_2 = -3.2, \kappa = 15$ and $\delta = -1.2$. Set $B : a = 1.2, b = -1.2, \sigma_1 = 0.4, \sigma_2 = -0.5, \kappa = 16$ and $\delta = 2.2$.

In order to run the simulations successfully, we take into account the starting condition at time zero (t=0) as per [5]:

$$q(x,0) = \text{Atanh}\left(\frac{\kappa}{2}x\right)e^{i(\delta x+\omega)}, \qquad (27)$$

where:

$$
\begin{aligned}
A &= \frac{\sqrt{6}b\kappa}{2\sqrt{-(\sigma_1+2\sigma_2)}},\\
\omega = \tfrac{\kappa}{2}\left(\kappa^2 + 6\delta^2\right) &\text{ and } \lambda = \tfrac{\delta}{\kappa}\left(3a\omega - 8\kappa\delta^2\right). \qquad (28)
\end{aligned}
$$

Taking the inherent constraint:

$$\sigma_1 + 2\sigma_2 < 0. \qquad (29)$$

Now, we present the results of the dark soliton simulation corresponding to these two cases:

- In Table 1, we consider a choice of t values and compare them to the exact solution for parameter Set A. For the same situation and with the same parameters, 2D simulations for values ranging from t=0.1,0.2,0.3,0.5 and the 3D soliton profile and contour plot of the approximate solution are shown in Figs. 1 and 2, correspondingly.
- In Table 2, we consider a choice of t values and compare them to the exact solution for parameter Set B. For the same situation and with the same parameters, 2D simulations for values ranging from t=0.1,0.2,0.3,0.5 and the 3D soliton profile and contour plot of the approximate solution are shown in Figs. 3 and 4, correspondingly.

The result of the simulation of the soliton correponding to the set of parameters A can be seen in Appendix A.

4.2. Pure-Cubic Bright Solitons

Consider the following cases of Eq. (1) with the given set of parameters: Set C: $a = 2.2, b = 1.1, \sigma_1 = 3.3, \sigma_2 = -0.2, \kappa = 17$ and $\delta = -1.0$. Set $D : a = 0.3, b = 2.2, \sigma_1 = -0.1, \sigma_2 = 3.1, \kappa = 18$ and $\delta = -0.2$.

In order to run the simulations successfully, we take into account the starting condition at time zero (t=0) as per [5]:

$$q(x,0) = B\,\text{sech}\left(\frac{\kappa}{2}x\right)e^{i(\delta x+\omega)}, \qquad (30)$$

where:

$$
\begin{aligned}
B &= \frac{\sqrt{6}b\kappa}{\sqrt{\sigma_1+2\sigma_2}},\\
\omega = \tfrac{\kappa}{2}\left(3\delta^2 - \kappa^2\right) &\quad \text{and} \quad \lambda = \tfrac{\delta}{\kappa}\left(3a\omega - 8\kappa\delta^2\right). \qquad (31)
\end{aligned}
$$

Taking the inherent constraint:

$$\sigma_1 + 2\sigma_2 > 0, \qquad (32)$$

Now, we present the results of the dark soliton simulation corresponding to these two cases:

- In Table 3, we consider a choice of t values and compare them to the exact solution for parameter Set C. For the same situation and with the same parameters, 2D simulations for values ranging from t=0.1,0.2,0.3,0.5 and the 3D soliton profile and contour plot of the approximate solution are shown in Figs. 5 and 6, correspondingly.
- In Table 4, we consider a choice of t values and compare them to the exact solution for parameter Set D. For the same situation and with the same parameters, 2D simulations for values ranging from t=0.1,0.2,0.3,0.5 and the 3D soliton profile and contour plot of the approximate solution are shown in Figs. 7 and 8, correspondingly.

4.3. Graphical View

Some solutions for Eq. (1) were derived by assigning particular values to the parameters of the system, categorized as sets A, B, C, and D. The solutions encompass both dark solitons and bright solitons. The solutions produced in this

Table 1. The absolute error when t=0.1, t=0.2, t=0.3 and t=0.50 for the case of parameter Set A and choosing K=12.

x	error when $t = 0.1$	error when $t = 0.2$	error when $t = 0.3$	error when $t = 0.5$
-1.00	1.6×10^{-7}	2.1×10^{-7}	3.4×10^{-7}	6.6×10^{-7}
-0.50	7.6×10^{-8}	1.4×10^{-7}	3.1×10^{-7}	5.1×10^{-7}
0.00	3.0×10^{-8}	4.5×10^{-8}	3.3×10^{-7}	4.6×10^{-7}
0.50	7.8×10^{-8}	1.6×10^{-7}	3.8×10^{-7}	6.1×10^{-7}
1.00	1.4×10^{-7}	2.4×10^{-7}	4.1×10^{-7}	7.5×10^{-7}

Table 2. The absolute error when t=0.1, t=0.2, t=0.3 and t=0.50 for the case of parameter Set B and choosing K=14.

x	error when $t = 0.1$	error when $t = 0.2$	error when $t = 0.3$	error when $t = 0.5$
-1.00	3.3×10^{-8}	3.9×10^{-8}	5.1×10^{-8}	7.7×10^{-7}
-0.50	2.3×10^{-9}	1.9×10^{-8}	3.6×10^{-8}	5.5×10^{-7}
0.00	1.1×10^{-9}	2.2×10^{-9}	2.6×10^{-8}	5.0×10^{-7}
0.50	2.0×10^{-9}	7.6×10^{-9}	4.1×10^{-8}	5.9×10^{-7}
1.00	3.5×10^{-8}	3.8×10^{-8}	5.2×10^{-8}	6.9×10^{-7}

study are novel, and the model is being examined for the first time using the proposed technique. We have shown 2D and 3D graphics to illustrate the features of a few simulated solutions. Graphs 2 and 4 depict the presence of two dark solitons as described by Eq. (1) . Plots 1 and 3 illustrate the temporal evolution of these solitons at various values of t. Graphs 6 and 8 illustrate two bright solitons of Eq. (1), while their temporal evolutions are depicted in graphs 5 and 7. The findings of this study illustrate the ability to achieve various solitary wave solutions in optical fibers by successfully handling the dispersive effects and nonlinearities. These solutions are capable of maintaining their form and speed during propagation. The acquisition of such solitons yields significant insights for the application of practical engineering in the field of fiber optic communication. All the computational work is accomplished by using Mathematica 12.2 version software.

5. Conclusions

The current paper displayed the pure-cubic bright and dark optical solitons that are recovered from the NLSE by the application of the LADM scheme. The error measure is strikingly small. The results included the surface plots and the contour plots as well for both kinds of solitons. Additionally, the two-dimensional plots showed that the match with the exact soliton solutions to the model is exact. The results carry a formidable future. Later, the model will be studied with power-law form of SPM followed by additional structures of it [2]. The analytical results are going to be first reported followed by the numerical scheme by LADM.

In future, the model will be taken up with birefringent fibers where the LADM will be applied to recover the bright and dark solitons there using the LADM scheme. Thereafter, the study will naturally extend with DWDM topology. Moreover, additional and yet powerful numerical schemes will be implemented. They are the variational iteration scheme, finite element method, finite difference method and other such schemes. This would lead to a contrast with the range of such implemented schemes. Such comparative studies exhibit the efficiency of the schemes applied to the photonics world!

Declaration of competing interest

The authors declare that they have no known competing financial interests or personal relationships that could be perceived as having influenced the work described in this paper.

References

[1] R. Y. Chiao, E. Garmire, and C. H. Townes, (1964) *"Self-trapping of optical beams"* **Physical review letters *13***: 479. DOI: 10.1103/PhysRevLett.13.479.

[2] P. Albayrak, M. Ozisik, M. Bayram, A. Secer, S. E. Das, A. Biswas, Y. Yıldırım, M. Mirzazadeh, and A. Asiri, (2023) *"Pure-Cubic Optical Solitons and Stability Analysis with Kerr Law Nonlinearity"* **Contemporary Mathematics *4***(3): 530–548. DOI: 10.37256/cm.4320233308.

[3] D. Lu, A. R. Seadawy, J. Wang, M. Arshad, and U. Farooq, (2019) *"Soliton solutions of the generalised third-order nonlinear Schrödinger equation by two mathematical methods and their stability"* **Pramana *93***: 44. DOI: 10.1007/s12043-019-1804-5.

Table 3. The absolute error when t=0.1, t=0.2, t=0.3 and t=0.50 for the case of parameter Set C and choosing K=12.

x	error when $t = 0.1$	error when $t = 0.2$	error when $t = 0.3$	error when $t = 0.5$
-1.00	1.1×10^{-7}	2.0×10^{-7}	3.2×10^{-7}	6.4×10^{-7}
-0.50	7.4×10^{-8}	1.6×10^{-7}	3.7×10^{-7}	5.9×10^{-7}
0.00	2.0×10^{-8}	3.3×10^{-8}	3.0×10^{-7}	4.2×10^{-7}
0.50	7.6×10^{-8}	1.9×10^{-7}	3.5×10^{-7}	5.8×10^{-7}
1.00	1.3×10^{-7}	2.2×10^{-7}	3.8×10^{-7}	6.6×10^{-7}

Table 4. The absolute error when t=0.1, t=0.2, t=0.3 and t=0.50 for the case of parameter Set D and choosing K=14.

x	error when $t = 0.1$	error when $t = 0.2$	error when $t = 0.3$	error when $t = 0.5$
-1.00	3.6×10^{-8}	4.1×10^{-8}	5.2×10^{-8}	7.8×10^{-7}
-0.50	2.2×10^{-9}	1.6×10^{-8}	3.0×10^{-8}	5.6×10^{-7}
0.00	2.4×10^{-9}	3.2×10^{-9}	2.1×10^{-8}	5.0×10^{-7}
0.50	2.0×10^{-9}	2.0×10^{-8}	3.1×10^{-8}	5.5×10^{-7}
1.00	3.8×10^{-8}	3.9×10^{-8}	5.4×10^{-8}	7.0×10^{-7}

[4] N. Nasreen, A. R. Seadawy, D. Lu, and W. A. Albarakati, (2019) *"Dispersive solitary wave and soliton solutions of the gernalized third order nonlinear Schrödinger dynamical equation by modified analytical method"* **Results in Physics *15***: 102641. DOI: 10.1016/j.rinp.2019.102641.

[5] S. Malik, S. Kumar, K. S. Nisar, and C. A. Saleel, (2021) *"Different analytical approaches for finding novel optical solitons with generalized third-order nonlinear Schrödinger equation"* **Results in Physics *29***: 104755. DOI: 10.1016/j.rinp.2021.104755.

[6] M. T. Islam, F. A. Abdullah, and J. Gómez-Aguilar, (2022) *"A variety of solitons and other wave solutions of a nonlinear Schrödinger model relating to ultra-short pulses in optical fibers"* **Optical and Quantum Electronics *54***: 866. DOI: 10.1007/s11082-022-04249-8.

[7] H. M. Baskonus, M. Younis, M. Bilal, U. Younas, Shafqat-ur-Rehman, and W. Gao, (2020) *"Modulation instability analysis and perturbed optical soliton and other solutions to the Gerdjikov-Ivanov equation in nonlinear optics"* **Modern Physics Letters B *34***: 2050404. DOI: 10.1142/S0217984920504047.

[8] J. Ahmad, S. Akram, S. U. Rehman, N. B. Turki, and N. A. Shah, (2023) *"Description of soliton and lump solutions to M-truncated stochastic Biswas–Arshed model in optical communication"* **Results in Physics *51***: 106719. DOI: 10.1016/j.rinp.2023.106719.

[9] T. A. Sulaiman, U. Younas, M. Younis, J. Ahmad, S. U. Rehman, M. Bilal, and A. Yusuf, (2022) *"Modulation instability analysis, optical solitons and other solutions to the (2+ 1)-dimensional hyperbolic nonlinear Schrodinger's equation"* **Computational Methods for Differential Equations *10***: 179–190. DOI: 10.22034/cmde.2020.38990.1711.

[10] S. Rehman, M. Bilal, M. Inc, U. Younas, H. Rezazadeh, M. Younis, and S. Mirhosseini-Alizamini, (2022) *"Investigation of pure-cubic optical solitons in nonlinear optics"* **Optical and Quantum Electronics *54***: 400. DOI: 10.1007/s11082-022-03814-5.

[11] J. K. Ghosh, P. Majumdar, and U. Ghosh, (2021) *"Qualitative analysis and optimal control of an SIR model with logistic growth, non-monotonic incidence and saturated treatment"* **Mathematical Modelling of Natural Phenomena *16***: 13. DOI: 10.1051/mmnp/2021004.

[12] K. Hosseini, M. Osman, M. Mirzazadeh, and F. Rabiei, (2020) *"Investigation of different wave structures to the generalized third-order nonlinear Scrödinger equation"* **Optik *206***: 164259. DOI: 10.1016/j.ijleo.2020.164259.

[13] D. Zhao, D. Lu, and M. M. Khater, (2022) *"Ultrashort pulses generation's precise influence on the light transmission in optical fibers"* **Results in Physics *37***: 105411. DOI: 10.1016/j.rinp.2022.105411.

[14] G. Adomian and R. Rach, (1986) *"On the solution of nonlinear differential equations with convolution product nonlinearities"* **Journal of mathematical analysis and applications *114***: 171–175. DOI: 10.1016/0022-247X(86)90074-0.

[15] G. Adomian. *Solving frontier problems of physics: the decomposition method*. Kluwer Academic Publishers, Boston MA, 1994.

Appendix a

$$
\begin{aligned}
q(x,t) \approx\ & q_0(x,t)+q_1(x,t)+q_2(x,t)+\cdots+q_{12}(x,t)\\
=\ & \frac{e^{x^2}t^4x^8}{13024}-\frac{1}{198}e^{\frac{3x^2}{2}}t^4x^8-\frac{1}{144}e^{2x^2}t^4x^8+\frac{1}{3}e^{x^2}it^3x^8+\frac{1}{13}e^{\frac{3x^2}{2}}it^3x^8-\frac{1}{16}e^{x^2}t^2x^9\\
& +\frac{9}{128}e^{\frac{x^2}{2}}itx^8+\frac{x^8}{344}-\frac{e^{\frac{x^2}{2}}t^4x^8}{108}+\left(\frac{1}{563}+\frac{i}{1342}\right)e^{x^2}t^4x^6-\left(\frac{1}{37}+\frac{i}{708}\right)e^{\frac{5x^2}{2}}t^6x^{10}\\
& -\frac{1}{53}e^{2x^2}t^4x^{12}-\left(\frac{1}{24}-\frac{7i}{2}\right)e^{x^2}t^3x^6+\left(\frac{1}{25}+\frac{i}{6}\right)e^{\frac{3x^2}{7}}t^8x^9+\frac{1}{6}e^{\frac{x^2}{2}}it^3x^6-2ie^{\frac{x^{11}}{2}}t\\
& -\left(\frac{1}{8}+\frac{5i}{7}\right)e^{x^2}t^2x^6+\frac{3}{138}e^{\frac{x^2}{2}}it^2x^6+\frac{9}{178}e^{\frac{x^2}{2}}itx^6-\frac{x^6}{23}-\frac{3e^{\frac{x^9}{5}}t^4x^6}{12}+\frac{13t^2}{23}\\
& +\left(\frac{5}{1105}+\frac{3i}{718}\right)e^{x^2}t^{12}x^4-\left(\frac{1}{18}+\frac{3i}{68}\right)e^{\frac{3x^2}{2}}t^4x^4-\frac{1}{4}e^{2x^2}t^4x^{11}-\left(\frac{1}{6}-\frac{23i}{96}\right)e^{x^2}t^3x^{12}\\
& +\left(\frac{1}{24}+\frac{i}{16}\right)e^{\frac{5x^2}{2}}t^3x^4+\frac{7}{32}e^{\frac{x^2}{2}}it^3x^5-\left(\frac{1}{6}+\frac{3i}{64}\right)e^{x^8}t^2x^{11}-\left(\frac{3}{32}-\frac{23i}{7}\right)e^{\frac{x^6}{2}}t^2x^4\\
& +\frac{7}{2}e^{\frac{x^2}{2}}t^2x^4-\frac{5}{12}itx^4+\frac{x^4}{3}-\frac{315e^{\frac{x^2}{2}}t^4x^4}{108}+\left(\frac{5}{1053}+\frac{7i}{184}\right)e^{x^2}t^4x^2-\frac{72e^{\frac{x^2}{2}}t^4}{926}\\
& -\left(\frac{1}{24}x+\frac{3i}{256}\right)e^{\frac{3x^2}{2}}t^4x^2-\frac{1}{37}e^{2x^2}t^4x^2+\left(\frac{13}{16}+\frac{i}{96}\right)e^{x^2}t^3x^2+\left(\frac{1}{392}+\frac{15i}{2}\right)e^{\frac{x^2}{2}}t^3x^2\\
& +\left(\frac{1}{48}+\frac{i}{8}\right)e^{\frac{3x^2}{2}}t^3x^7+\left(\frac{21}{32}+\frac{21i}{33}\right)e^{\frac{x^2}{2}}t^2x^{10}+\frac{1}{4}e^{x^2}it^2x^2-ie^{\frac{x^2}{2}}tx^2-\frac{3}{7}itx^2-\frac{x^2}{4}\\
& -\frac{5e^{\frac{x^2}{2}}t^4x^2}{204}+\left(\frac{5}{708}+\frac{i}{206}\right)e^{x^2}t^4-\left(\frac{1}{9}+\frac{i}{56}\right)e^{\frac{3x^2}{2}}t^4-\frac{1}{14}e^{2x^2}t^4-\frac{6it}{4}\\
& +\left(\frac{5}{3}-\frac{i}{2}\right)e^{x^2}t^3+\left(\frac{1}{172}+\frac{5i}{13}\right)e^{\frac{x^2}{2}}t^3+\left(\frac{1}{4}-\frac{i}{5}\right)e^{\frac{x^2}{2}}t^2+\frac{e^{6x}t^8x^{10}}{113}-\frac{7e^{\frac{x^5}{2}}t^6x^{12}}{952}\\
& \frac{x}{614}(1-1506x^2+152x^4t^6-13x^6+x^8t^{10}+\left(\frac{4}{21}-\frac{3i}{8}\right)e^{\frac{x^8}{7}}t^2x^4-16x^6+9x^8t^{10}+7x^{12}t^8)\\
& +\frac{x}{648}[12t^4e^{x^2}\left(452x^2+(90e^{\frac{x^2}{2}}+19)x^8+16(2e^{\frac{x^2}{5}}+72)x^6+(438e^{\frac{x^2}{2}}+134)x^4+208\right)\\
& +t^4e^{\frac{x^2}{2}}\left(95x^2+(1-150ie^{\frac{x^2}{2}}+192e^{\frac{3x^2}{2}})x^8+3(11-4104ie^{\frac{x^2}{2}})x^6+9(13-76ie^{\frac{x^2}{2}})x^4+7\right)\\
& -7it^3e^{\frac{x^2}{2}}\left((8-3e^{\frac{x^2}{2}})x^2+(12e^{x^2}+3)x^8-3(28e^{\frac{x^2}{2}}+8e^{x^2}-7)x^6+(71-144e^{\frac{x^2}{2}})x^4+23\right)\\
& -316t^2\left(2e^{x^2}(19x^4-41x^2+32)x^4+e^{\frac{x^2}{2}}(6x^8+101x^6+1421x^4-268x^2+102)+17\right)\\
& -206it\left(7(17e^{\frac{x^2}{2}}+12)x^2+22e^{\frac{x^2}{2}}x^{12}-(56e^{\frac{x^2}{6}}+23)x^4+\frac{7i}{78}e^{x^2}t^{12}+16\right)].
\end{aligned}
$$

[16] J.-S. Duan, (2011) *"Convenient analytic recurrence algorithms for the Adomian polynomials"* **Applied Mathematics and Computation *217***: 6337–6348. DOI: 10.1016/j.amc.2011.01.007.

[17] A.-M. Wazwaz, (2005) *"Adomian decomposition method for a reliable treatment of the Emden–Fowler equation"* **Applied Mathematics and Computation *161***: 543–560. DOI: 10.1016/j.amc.2003.12.048.

[18] J. Biazar and R. Islam, (2004) *"Solution of wave equation by Adomian decomposition method and the restrictions of the method"* **Applied Mathematics and Computation *149***: 807–814. DOI: 10.1016/S0096-3003(03)00186-3.

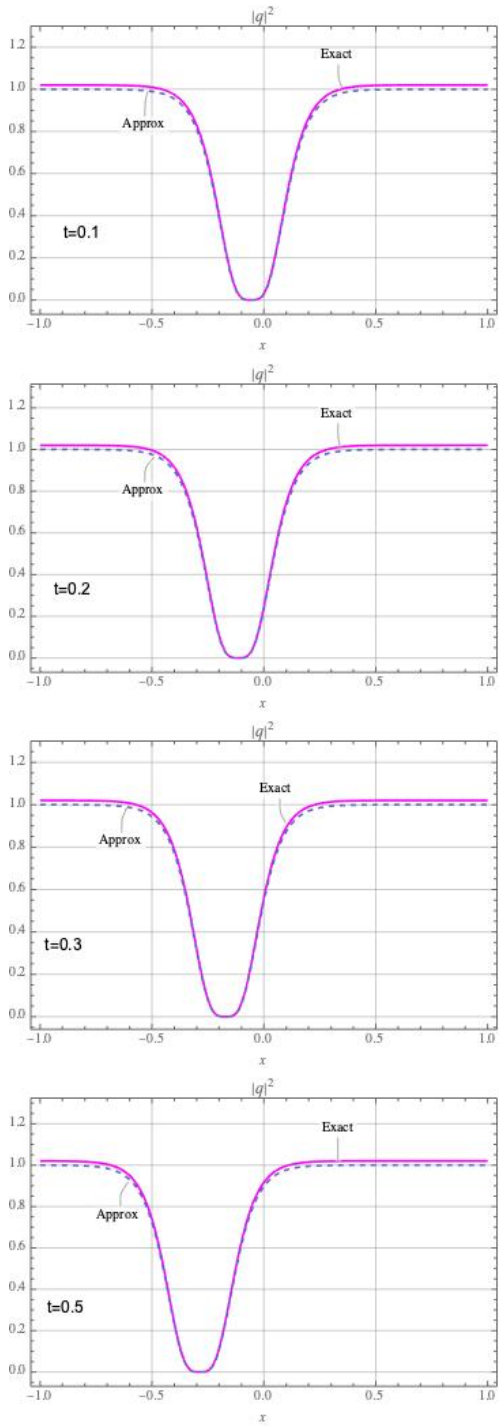

Fig. 1. LADM and exact solution comparison for $-1 \leq x \leq 1$ and t=0.1,0.2,0.3,0.5. Case of parameter Set A with K=12.

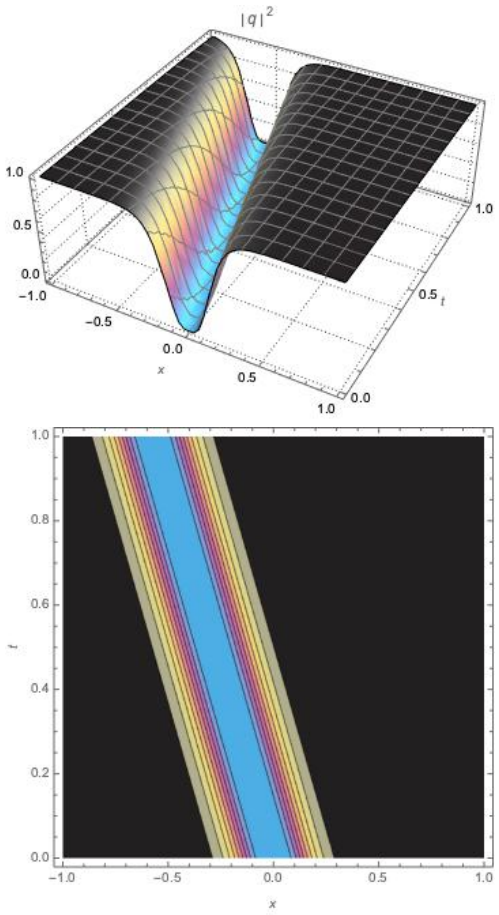

Fig. 2. 3D profile of the solution $|q(x,t)|^2$ for the case of the parameter Set A (above). 2D contour plot of the dark soliton solution with the same parameter (below).

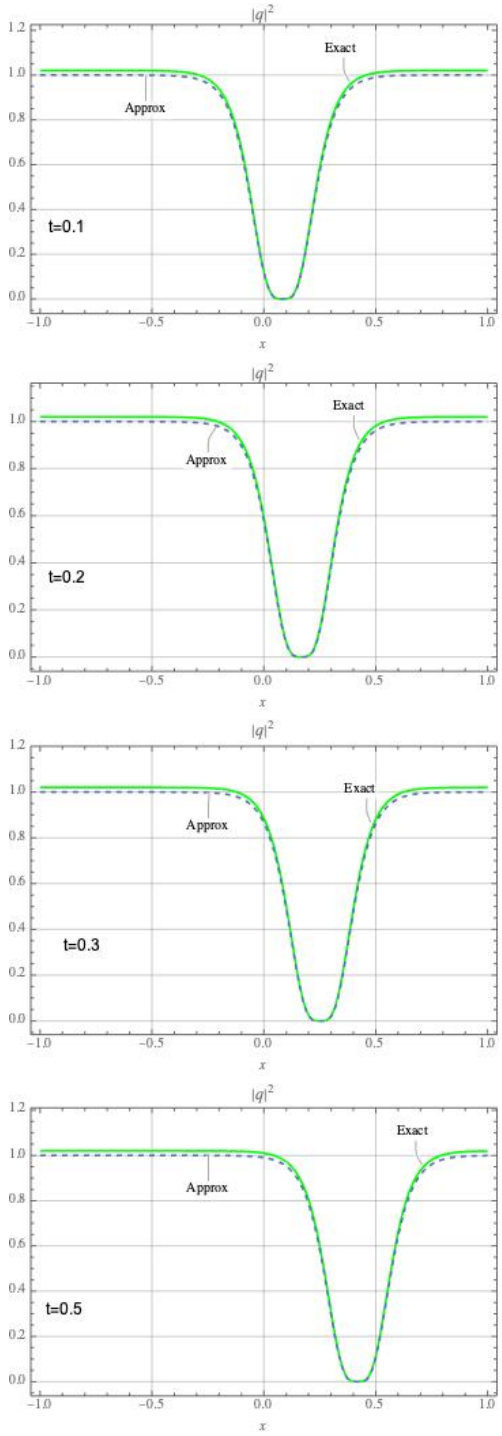

Fig. 3. LADM and exact solution comparison for $-1 \leq x \leq 1$ and t=0.1,0.2,0.3,0.5. Case of parameter Set B with K=14.

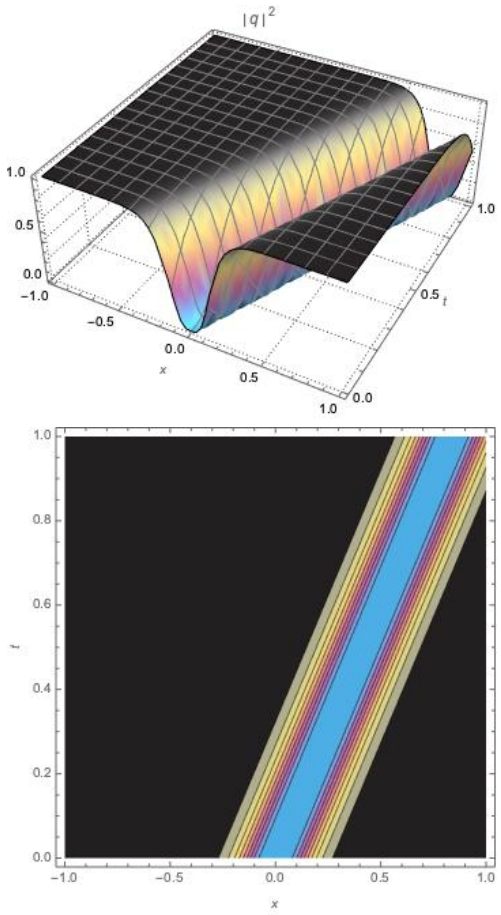

Fig. 4. 3D profile of the solution $|q(x,t)|^2$ for the case of the parameter Set B (above). 2D contour plot of the dark soliton solution with the same parameter (below).

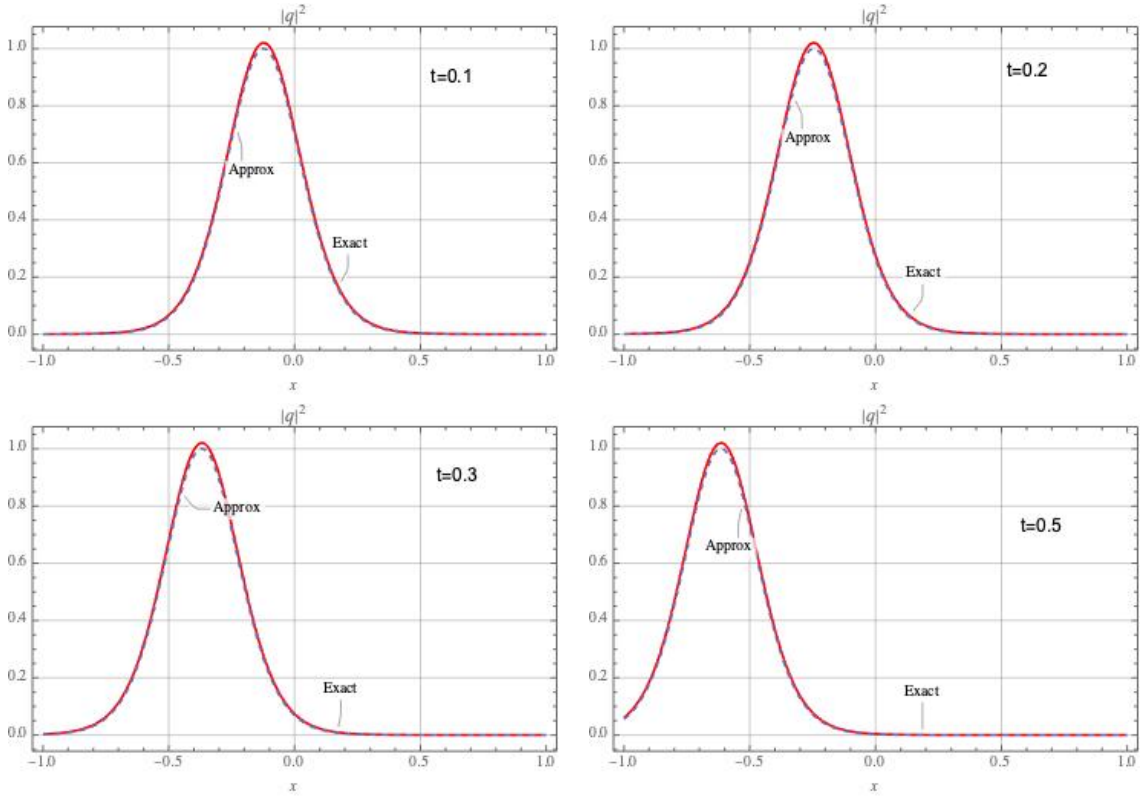

Fig. 5. LADM and exact solution comparison for $-1 \leq x \leq 1$ and t=0.1,0.2,0.3,0.5. Case of parameter Set C with K=12.

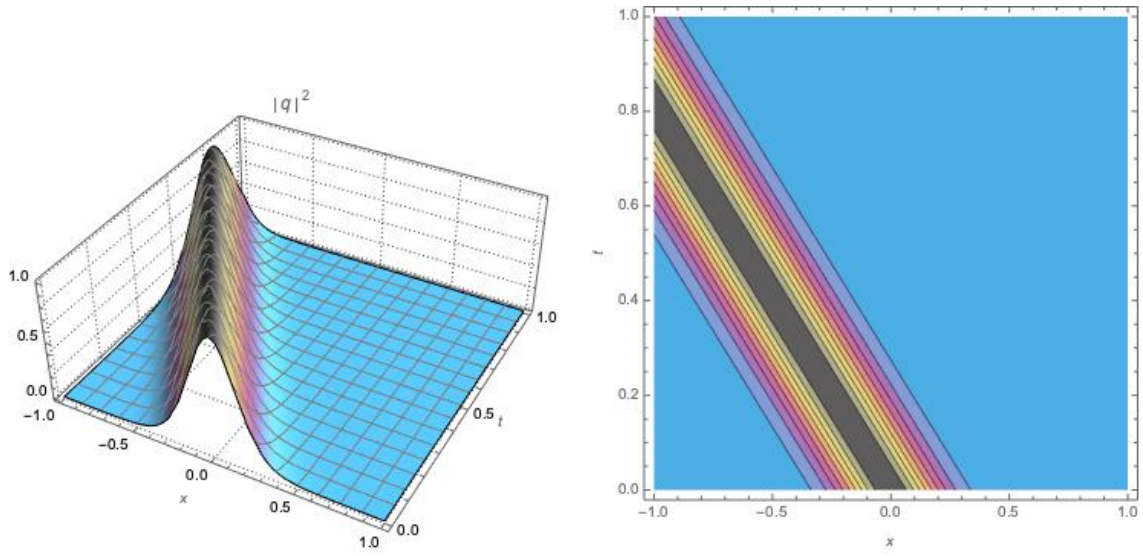

Fig. 6. 3D profile of the solution $|q(x,t)|^2$ for the case of the parameter Set C (above). 2D contour plot of the bright soliton solution with the same parameter (below).

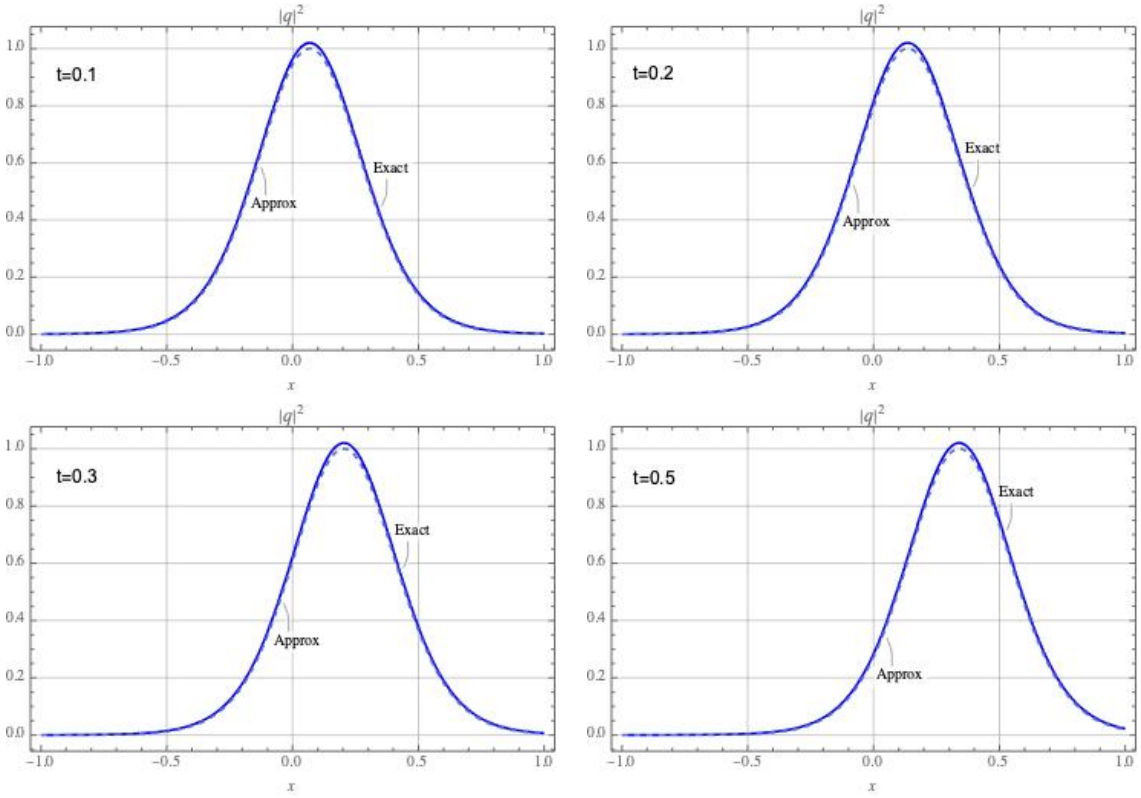

Fig. 7. LADM and exact solution comparison for $-1 \leq x \leq 1$ and t=0.1,0.2,0.3,0.5. Case of parameter Set D with K=14.

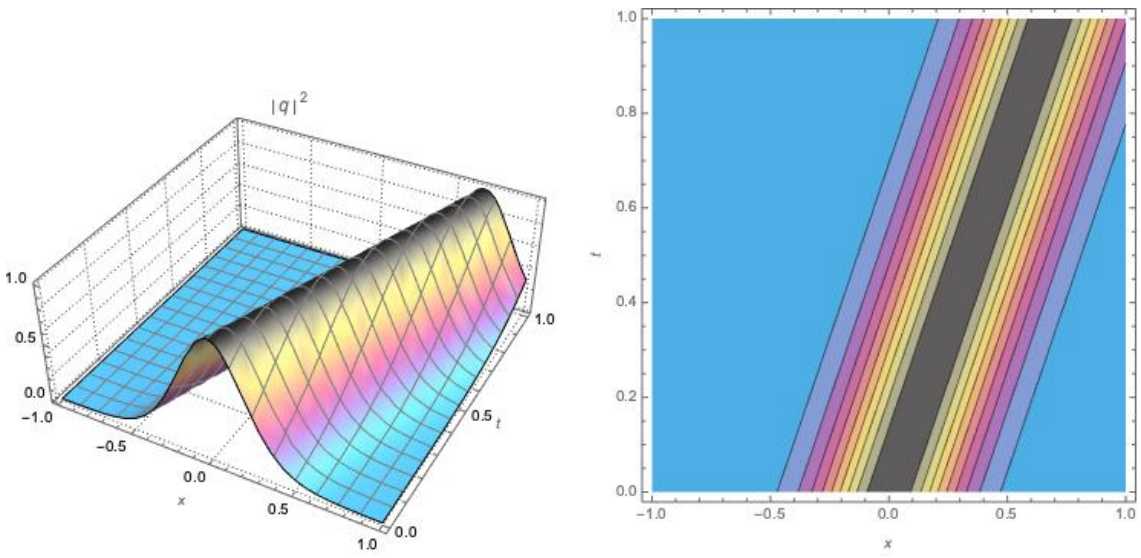

Fig. 8. 3D profile of the solution $|q(x,t)|^2$ for the case of the parameter Set D (above). 2D contour plot of the bright soliton solution with the same parameter (below).